

LETTERS

Self-Assembled Nanowire–Nanoribbon Junction Arrays of ZnO

Puxian Gao

*Center for Nanoscience and Nanotechnology, School of Materials Science and Engineering,
Georgia Institute of Technology, Atlanta, Georgia 30332-0245*

Zhong Lin Wang*

*School of Materials Science and Engineering, and School of Chemistry and Biochemistry,
Georgia Institute of Technology, Atlanta, Georgia 30332-0245*

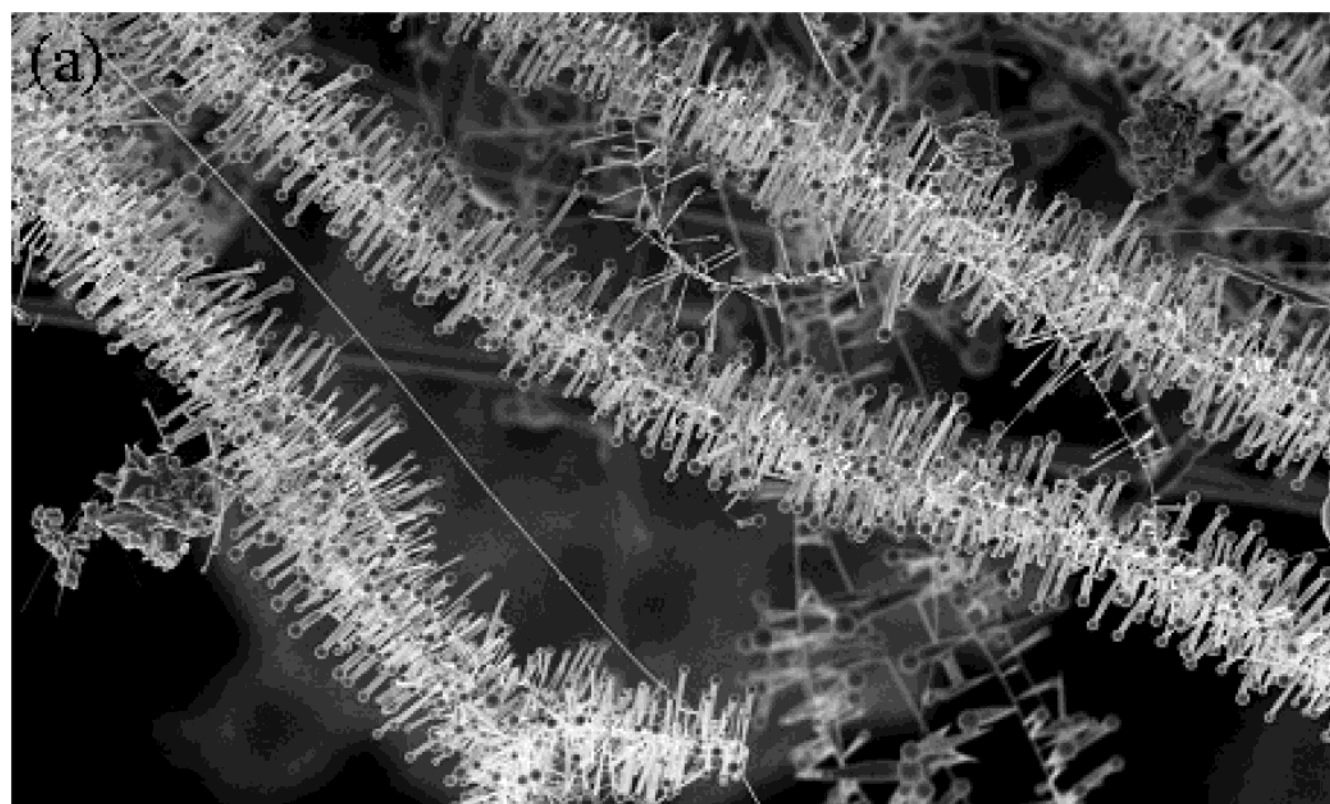
Received: July 16, 2002; In Final Form: August 27, 2002

We report the synthesis and characterization of nanowire–nanoribbon junction arrays of ZnO, which were grown by thermal evaporation of the mixture of ZnO and SnO₂ powders at 1300 °C through a vapor–liquid–solid process. The Sn particles produced by the reduction of SnO₂ act as the catalyst; the structure is formed due to a fast growth of ZnO nanowires along [0001] and the subsequent “epitaxial” radial growth of the ZnO nanoribbons along the six $\langle 01\bar{1}0 \rangle$ directions around the nanowire. The “liana” shape nanostructure could be a candidate for fabricating ultrahigh sensitive sensors.

Semiconducting oxides, as an important series of materials candidates for optoelectronic devices and sensors, have attracted considerable attention in scientific research and technological applications. Recently, quasi-one-dimensional nanostructures for the functional materials have been successfully fabricated by using various approaches including thermal evaporation,^{1–3} sol–gel,⁴ arc discharge,⁵ laser ablation,⁶ and template-based method.⁷ To date, extensive research work has been focused on ZnO, which is one of the most useful oxides for optical and sensor applications. Many different morphological ZnO nanostructures, including wires¹, belts², and rods,⁸ etc., have been fabricated. In this letter, we report a new structural configuration of the ZnO: the self-assembled nanowire–nanoribbon junction arrays. Details will be presented about their synthesis, structure and growth mechanism.

Thermal evaporation^{1–3,9} was used in the present study for synthesis of ZnO nanostructures. The experimental setup consists of a horizontal high-temperature tube furnace of length ~50 cm, an alumina tube (~75 cm in length), a rotary pump system, and a gas controlling system. Commercial (Alfa Aesor) ZnO and SnO₂ powders with weight ratio of 1:1 (5 g in total) were fully mixed by grounding the powder mixture for 15 min and then used as the source material. The source material was loaded on an alumina boat and positioned at the center of the alumina tube. After evacuating the tube to 2×10^{-3} Torr, thermal evaporation was conducted at 1300 °C for 1 h under pressure of 300–400 Torr and Ar carrier gas flow rate of 50 sccm (standard cubic centimeters per minute). The synthesized nanostructures grew on the top of the innerwall of the alumina tube in a region of ~4 cm in width, located downstream ~15 cm away from the source material (located in the middle of the furnace), and the local growth temperature was in the range of 700~800 °C.

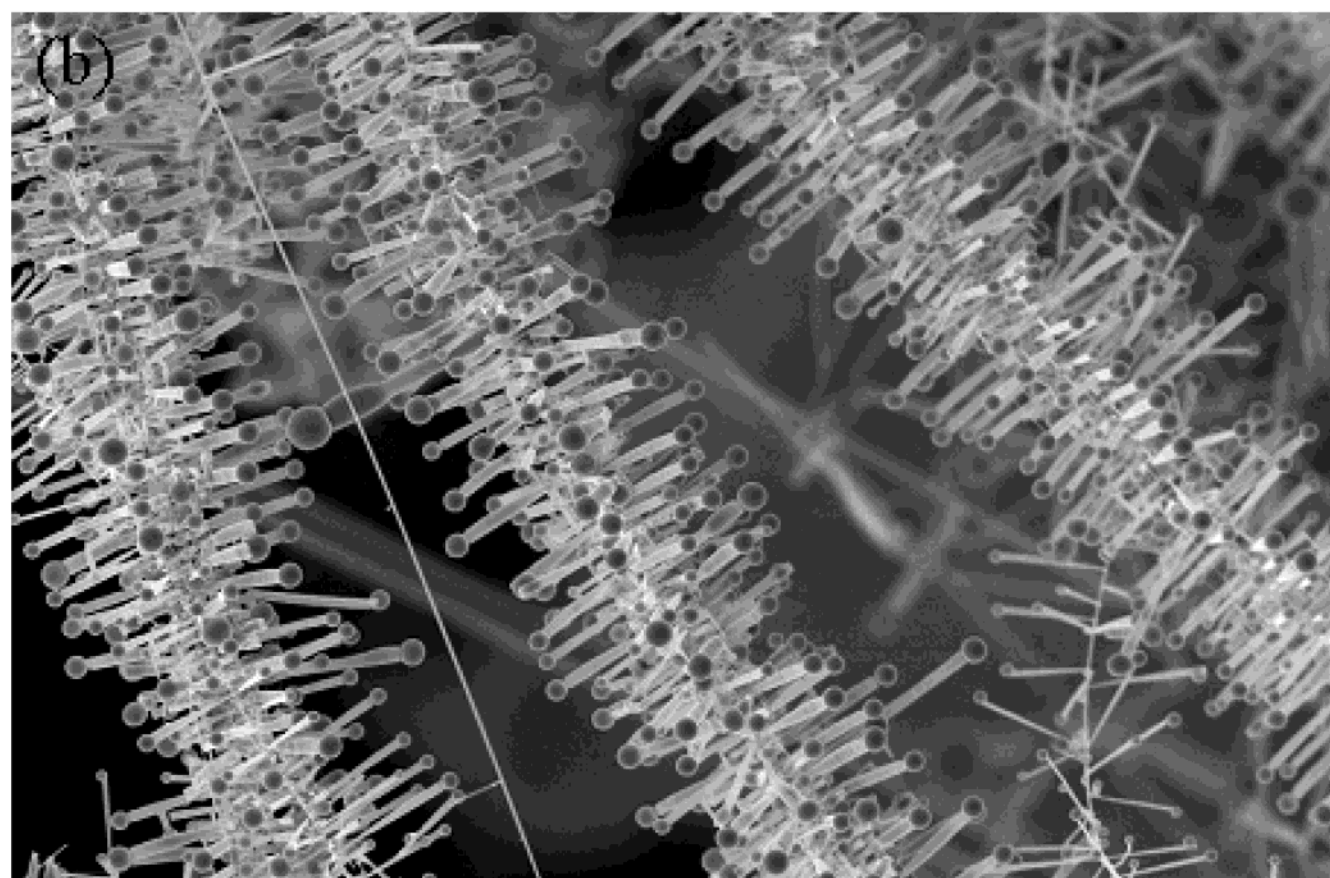
* Corresponding author. E-mail: zhong.wang@mse.gatech.edu.



Mag = 2.50 K X 

EHT = 5.00 kV
WD = 11 mm

Signal A = InLens
Photo No. = 6436
Date :11 Jul 2002
Time :0:36:28



Mag = 5.00 K X 

EHT = 5.00 kV
WD = 12 mm

Signal A = InLens
Photo No. = 6345
Date :8 Jul 2002
Time :15:31:41

Figure 1. SEM images of the as-synthesized ZnO nanostructures, showing strings of "tadpole-like" nanostructures.

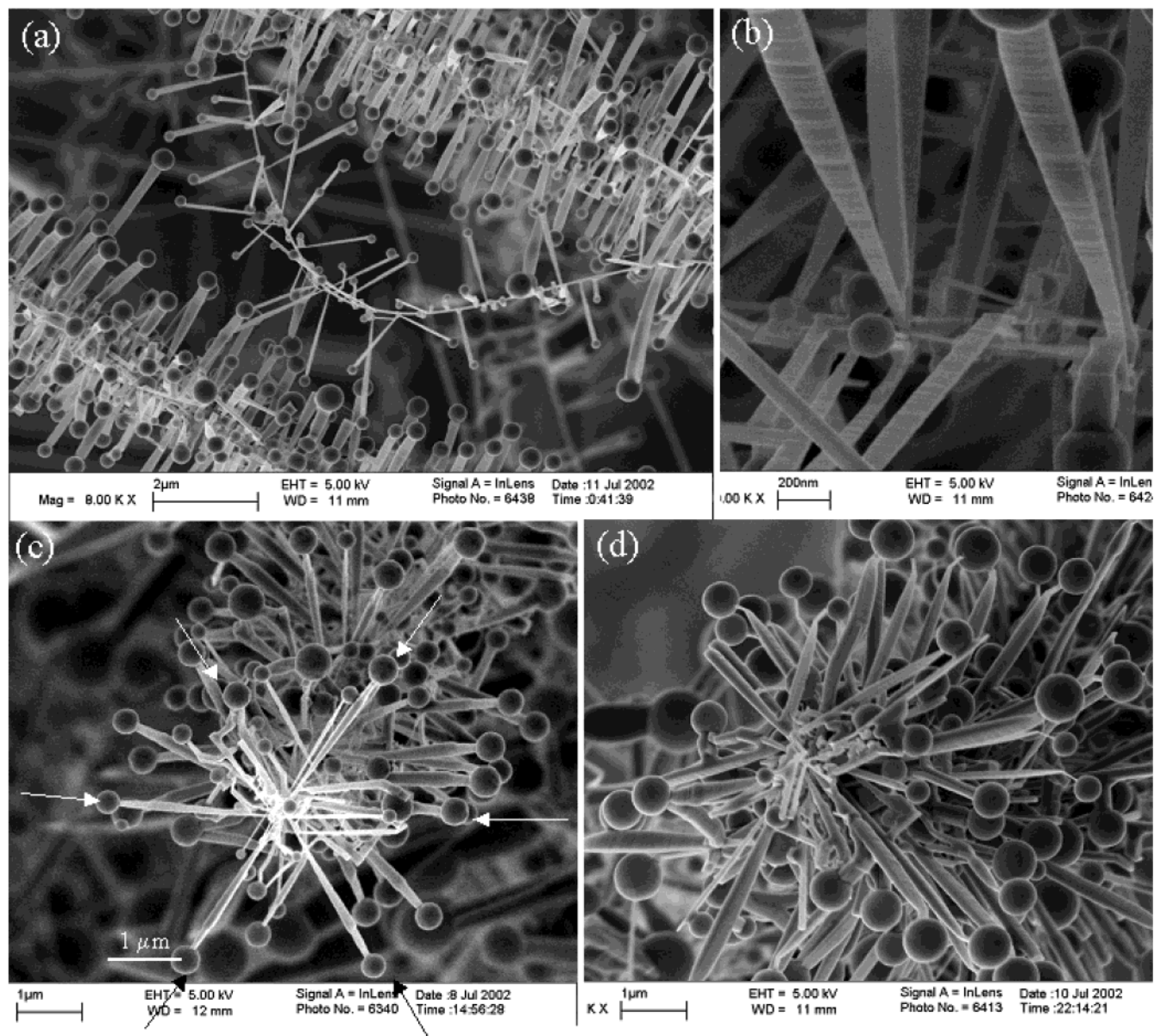


Figure 2. High magnification SEM images of the ZnO nanostructures showing (a, b) the ribbon shape of the “tadpole-like” nanostructure, (c, d) and their quasi-6-fold radial distribution around the axial nanowire.

The prepared products were characterized by high-resolution field emission scanning electron microscopy (FESEM) (LEO 1530 FEG at 5 & 10 kV), transmission electron microscopy (TEM) (JEOL 100 °C at 100 kV; field emission TEM Hitachi HF-2000 at 200 kV), and energy-dispersive X-ray spectroscopy (EDS) attached to the SEM and TEM, respectively.

The yield of the synthesis is reasonably high. Typical scanning electron microscopy (SEM) images of the as-synthesized products are given in Figure 1. Figure 1a shows a low-magnification image of the as-synthesized products with a uniform feature consisting of sets of central axial nanowires, surrounded by radial oriented “tadpole-like”¹⁰ nanostructures. The morphology of the string appears like a “liana”, and the axial nanowire is the “rattan”, which has a uniform cross section with dimension in the range of a few tens of nanometer. The “tadpole-like” branches have spherical balls at the tips (Figure 1b). EDS analysis shows that the tadpole-like structure and the central nanowire are ZnO, while the ball at the tip is Sn.

It is apparent in Figure 2a that the top and bottom strings have a dense and ordered stacking of tadpole-like nanostructures with maximum widths of ~ 300 nm, while the central one is a string assembled with sparsely distributed tadpole-like nanostructures along a thin nanowire. A high magnification SEM image given in Figure 2b shows the ribbon shape of the tadpole-like structures, with a fairly uniform thickness, and their surfaces are rough with steps. The contact point between the nanoribbon with the axial nanowire is rather small in the order of a few tens of nanometers, while far away from the contacting point, the nanoribbon size is rather large in the order of 100–200 nm.

An interesting phenomenon observed in Figure 2c is that the distribution of the nanoribbons around the axial nanowire has an angle interval of $\sim 60^\circ$. A typical front view of the nanowire indicates a 6-fold symmetrical ordered assembly (Figure 2d).

Figure 3a is a typical TEM image of the nanowire–nanoribbon junction structures. The axial nanowire is as thin as ~ 30 nm, while the width of the nanoribbon is rather large

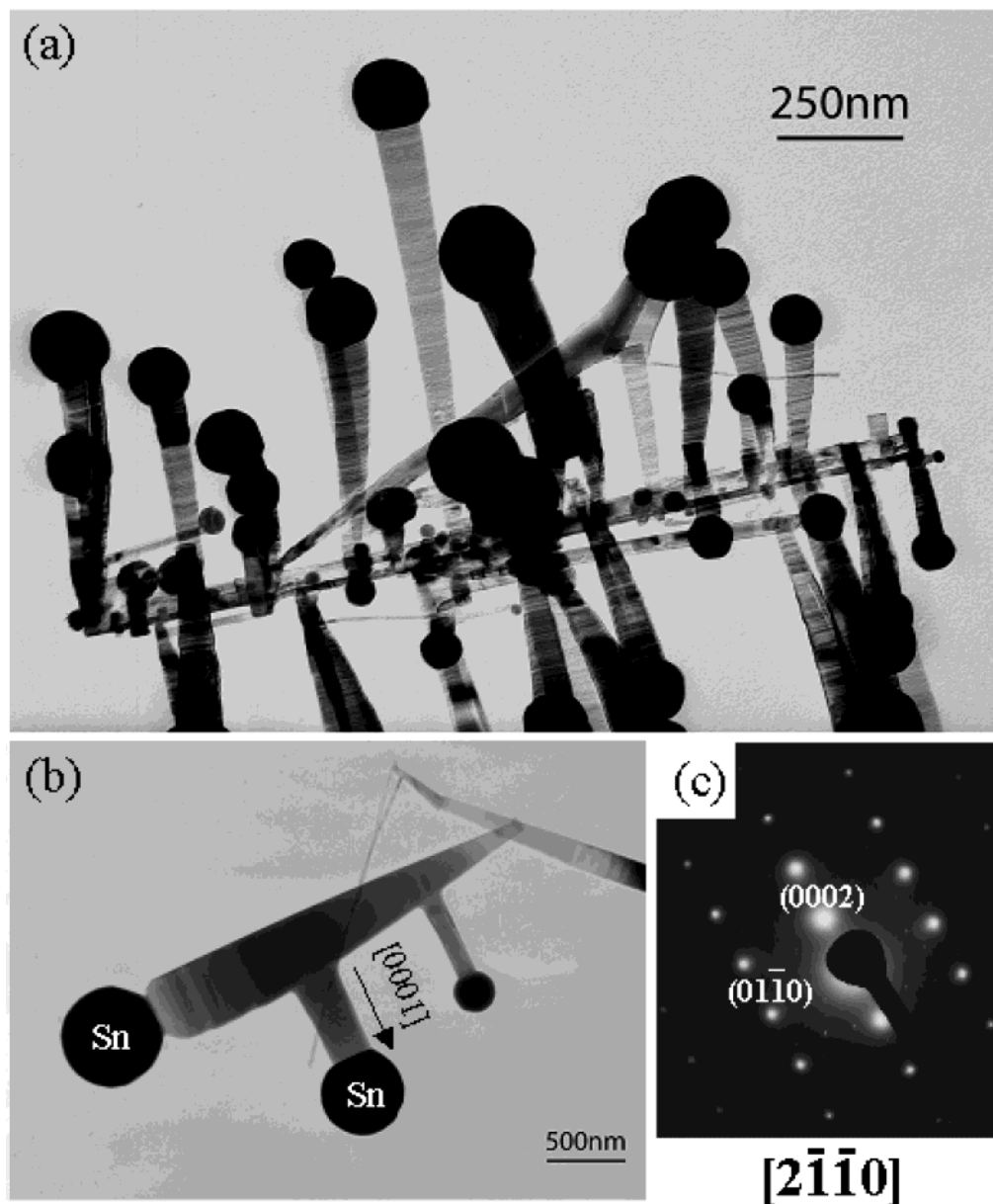


Figure 3. (a) Low-magnification TEM image of the as-synthesized ZnO nanowire–nanoribbon junction arrays. (b, c) TEM image of two junctions and the corresponding electron diffraction pattern.

and increases as the growth continues. The contrast introduced by the surface steps on the ribbons is apparent. Figure 3b shows a case that two nanowires grow from a nanoribbon. The TEM image and the corresponding electron diffraction pattern show that the nanoribbon and the nanowire have the wurzite (hexagonal) structure. The most commonly observed growth direction of the nanoribbons is $[01\bar{1}0]$ (and equivalent directions), and the nanowires are $[0001]$; the top surfaces of the nanoribbon are $\pm(2\bar{1}\bar{1}0)$.

Figure 4a shows a junction consisting of an axial nanowire and two branches of nanoribbons. The nanowire and nanoribbons are of the same crystal piece and they share a common $(2\bar{1}\bar{1}0)$ plane; their growth directions are $[0001]$ and $\pm[01\bar{1}0]$ (Figure 4b), respectively. Electron diffraction, bright and dark-field TEM images (Figure 4c,d) recorded from the junction area prove that the nanoribbon and nanowire have the same crystal structure and orientation.

In the present study, a mixture of SnO_2 and ZnO powders was used as the source material. It is known that SnO_2 can

decompose into Sn and O_2 at high temperature;^{11–14} thus, the growth of the nanowire–nanoribbon junction arrays is the result of vapor–liquid–solid (VLS) growth process,^{15–17} in which the Sn catalyst particles are responsible for initiating and leading the growth of ZnO nanowires and nanoribbons. Our previous study of ZnO nanobelts shows that the fast growth directions of ZnO are $[0001]$ and $\langle 10\bar{1}0 \rangle$.²

The growth of the novel structure presented in the present study can be separated into two stages. The first stage is a fast growth of the ZnO axial nanowire along $[0001]$ with Sn as the catalyst (Figure 5a). The growth rate is so high that a slow increase in the size of the Sn droplet has little influence on the diameter of the nanowire; thus, the axial nanowire has a fairly uniform shape along the growth direction.

The second stage of the growth is the nucleation and epitaxial growth of the nanoribbons due to the arrival of the tiny Sn droplets onto the ZnO nanowire surface (Figure 5b). This stage is much slower than the first stage because the lengths of the nanoribbons are uniform and much shorter than that of the

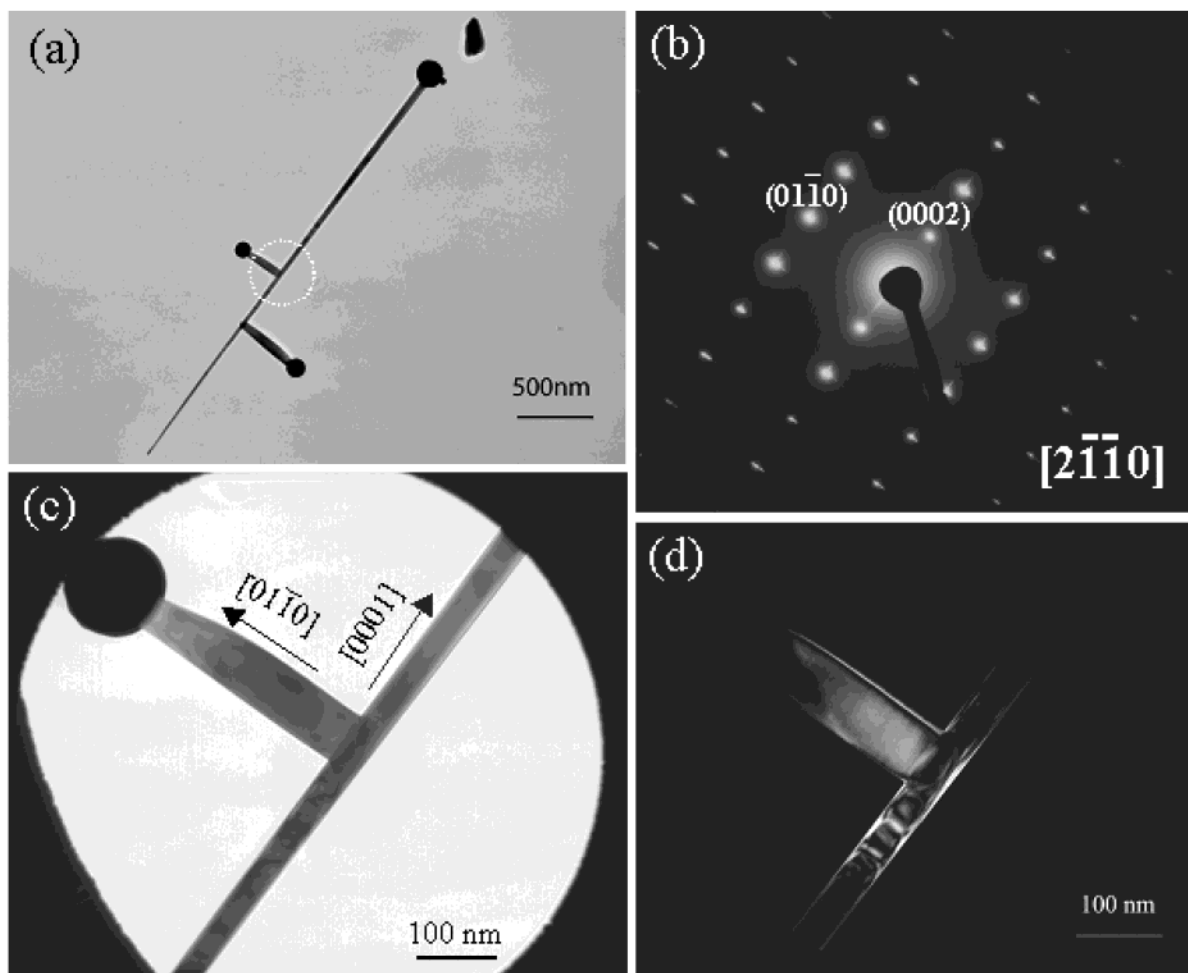


Figure 4. (a) TEM image of two junctions and (b) the corresponding electron diffraction pattern from the junction region as indicated by a white circle in (a) (excluding the Sn particle). (c, d) Bright-field and (0002) dark-field TEM images from the junction region.

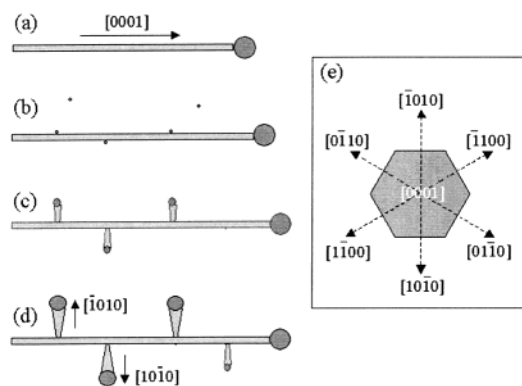


Figure 5. (a–d) Schematic diagram showing the two-stage growth of the ZnO junctions. (e) A cross-sectional model illustrating the isotropic epitaxial growth of the nanoribbons around the nanowire.

nanowire. Since Sn is in liquid state at the growth temperature, it tends to adsorb the newly arriving Sn species and grows into a larger size particle (i.e., coalescing) (Figure 5c). Therefore, the width of the nanoribbon increases as the size of the Sn particle at the tip becoming larger, resulting in the formation of the tadpole-like structure observed in TEM (Figure 5d).

The ZnO nanowire is likely to have a hexagonal cross section bounded by $\pm(10\bar{1}0)$, $\pm(01\bar{1}0)$, and $\pm(\bar{1}100)$, which are six crystallographic equivalent planes.^{1,2} The Sn liquid droplets

deposited onto the ZnO nanowire lead to the simultaneous growth of the ZnO nanoribbons along the six growth directions: $\pm[10\bar{1}0]$, $\pm[01\bar{1}0]$, and $\pm[\bar{1}100]$ (Figure 5e). The angles between the two adjacent growth directions is 60° , resulting in the 6-fold symmetric distribution of the nanoribbons around the nanowire, in agreement with the observation shown in Figure 2c,d.

In summary, by thermal evaporating a mixture of ZnO and SnO₂, self-assembled nanowire–nanoribbon junction arrays of ZnO have been synthesized. The growth is dominated by the VLS mechanism and Sn particles reduced from SnO₂ serve as the catalyst for the growth. The axial nanowires (the “rattans”) are the result of fast growth along [0001], and the surrounding “tadpole-like” nanoribbons are the growth along $\langle 10\bar{1}0 \rangle$. An isotropic growth along six $\langle 10\bar{1}0 \rangle$ results in the ordered radial distribution of the nanoribbons around the axial nanowire. The junction arrays of ZnO structures reported here are likely to have ultrahigh surface sensitivity due to the unique structure, and they are a candidate for building sensors with ultrahigh sensitivity.¹⁸ It may be possible that, through further adjustment of synthesis parameters including temperature, pressure, source composition, etc., more perfectly and orderly self-assembled junction arrays could be prepared.

Acknowledgment. Thanks to the financial support of the U.S. National Science Foundation Grant DMR-9733160, and the Georgia Tech Electron Microscopy Center for providing the research facility.

References and Notes

- (1) Huang, M. H.; Mao, S.; Feick, H.; Yan, H. Q.; Wu, Y. Y.; Kind, H.; Weber, E.; Russo, R.; Yang, P. D. *Science* **2001**, *292*, 1897.
- (2) Pan, Z. W.; Dai, Z. R.; Wang, Z. L. *Science* **2001**, *291*, 1947.
- (3) Dai, Z. R.; Gole, J. L.; Stout, J. D.; Wang, Z. L. *J. Phys. Chem. B* **2002**, *106*, 1274.
- (4) Krumeich, F.; Muhr, H. J.; Niederberger, M.; Bieri, F.; Schnyder, B.; Nesper, R. *J. Am. Chem. Soc.* **1999**, *121*, 8324.
- (5) Choi, Y. C.; Kim, W. S.; Park, Y. S.; Lee, S. M.; Bae, D. J.; Lee, Y. H.; Park, G. S.; Choi, W. B.; Lee, N. S.; Kim, J. M. *Adv. Mater.* **2000**, *12*, 746.
- (6) Tang, Y. H.; Zheng, Y. F.; Wang, N.; Bello, I.; Lee, C. S.; Lee, S. T. *Appl. Phys. Lett.* **1999**, *74*, 3824.
- (7) Satishkumar, B. C.; Govindaraj, A.; Ogel, E. M.; Basumallick, L.; Rao, C. N. R. *J. Mater. Res.* **1997**, *12*, 64.
- (8) Wu, J.-J.; Liu, S.-C. *Adv. Mater.* **2002**, *14*, 215.
- (9) Lee, S. T.; Wang, N.; Zhang, Y. F.; Tang, Y. H. *MRS Bull.* **1999**, *24*, 36.
- (10) Pan, Z. W.; Dai, Z. R.; Xu, L.; Lee, S. T.; Wang, Z. L. *J. Phys. Chem. B* **2001**, *105*, 2507.
- (11) Hoenig, C. L.; Searcy, A. W. *J. Am. Ceram. Soc.* **1966**, *49*, 128.
- (12) Kelly, K. K. *U. S. Bur. Mines Bull.* **1949**, *476*, 187.
- (13) Dai, Z. R.; Pan, Z. W.; Wang, Z. L. *J. Am. Chem. Soc.*, **2002**. In press.
- (14) Wang, Z. L.; Pan, Z. W. *Adv. Mater.* **2002**. In press.
- (15) Wagner, R. S.; Ellis, W. C. *Appl. Phys. Lett.* **1964**, *4*, 89.
- (16) Morales, A. M.; Lieber, C. M. *Science* **1998**, *279*, 208.
- (17) Pan, Z. W.; Dai, Z. R.; Ma, C.; Wang, Z. L. *J. Am. Chem. Soc.* **2002**, *124*, 1817.
- (18) Wang, Z. L.; Kang, Z. C. *Functional and Smart Materials—Structure Evolution and Structure Analysis*; Plenum Press: New York, 1998.